

# High-Pressure Synthesis and Structure of $\text{SrCo}_6\text{O}_{11}$ : Pillared Kagomé Lattice System with a 1/3 Magnetization Plateau

Shintaro Ishiwata,\* Dan Wang, Takashi Saito, and Mikio Takano

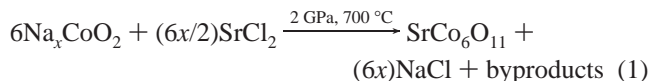
*Institute for Chemical Research (ICR),  
Kyoto University, Uji, Kyoto 611-0011, Japan*

Received March 25, 2005

Among layered transition metal oxides, considerable attention has been paid to cobalt oxides containing  $\text{Co}^{3+}/\text{Co}^{4+}$ -triangular lattices since the discovery of giant thermoelectricity in  $\text{Na}_x\text{CoO}_2$  and the subsequent discovery of exotic superconductivity in  $\text{Na}_{0.35}\text{CoO}_2 \cdot 1.3\text{H}_2\text{O}$ .<sup>1,2</sup> These unconventional properties are believed to arise from the nature of strongly correlated electrons hopping on a  $\text{Co}^{3+}/\text{Co}^{4+}$ -triangular lattice. It has been argued that the origin of these phenomena is related to the geometrical spin frustration suppressing a long-range magnetic ordering.<sup>3</sup> The triangular lattice of  $\text{Na}_x\text{CoO}_2$  consists of  $\text{CoO}_6$  octahedra, where the 3d levels are split into the 2-fold degenerate  $e_g$  (higher) levels and the 3-fold degenerate  $t_{2g}$  (lower) levels. Since the low spin state is preferred for  $\text{CoO}_6$  octahedra at low temperatures, the ground state of  $\text{Co}^{3+}$  is nonmagnetic, while  $\text{Co}^{4+}$  bears spin ( $S = 1/2$ ) and charge degrees of freedom.<sup>4</sup> To gain insight into these electronic properties, we have made a search for new  $\text{Co}^{3+}/\text{Co}^{4+}$ -layered cobalt oxides using  $\text{Na}_x\text{CoO}_2$  as a starting material.

High-pressure (HP) techniques are known to stabilize dense packing structures such as the perovskite structure.<sup>5</sup> For instance, the layered hexagonal phase of  $\text{La}_4\text{Cu}_3\text{MoO}_{12}$  prepared at ambient pressure is transformed into a three-dimensional perovskite phase at 6 GPa and 1200 °C.<sup>6</sup> On the other hand, soft chemical syntheses such as ion exchange reactions between alkali-containing layered compounds and chlorides are useful for designing new oxides.<sup>7–10</sup> In the present work, we combined these two synthetic strategies:

a mixture of  $\gamma\text{-Na}_x\text{CoO}_2$  and  $\text{SrCl}_2$  was treated under HP to synthesize cation-exchanged novel oxide,  $\text{SrCo}_6\text{O}_{11}$ , which is unavailable at ambient pressure.



As will be described below, the present cobalt oxide crystallizes in the *R*-type hexagonal ferrite structure, where two kinds of Co–O pillars, each forming a triangular lattice, intervene between the  $\text{Co}_3\text{O}_8$  Kagomé layers. We note here that hexagonal platelike single crystals such as that shown in Figure 1 can be obtained through another synthetic route, making use of the incongruent melting of an oxygen-deficient Ruddlesden–Popper phase,  $\text{Sr}_3\text{Co}_2\text{O}_{7-\delta}$  ( $\delta \sim 1$ ) (ref 11) under HP (see Supporting Information). Observation of a peculiar field- and orientation-dependence of magnetization using these crystals will also be described briefly.

Polycrystalline samples and single crystals were prepared with a conventional cubic anvil-type HP apparatus. The starting materials for the polycrystalline samples were  $\gamma\text{-Na}_x\text{CoO}_2$  ( $x \sim 0.5$ ) (ref 12),  $\text{SrCl}_2$ , and  $\text{KClO}_4$  (oxidizer) mixed in a molar ratio of 1:1:1. The oxidizer was indispensable for the suppression of byproducts such as  $\text{Co}_3\text{O}_4$ . The mixture was sealed in a gold capsule ( $\phi 4 \times 6$  mm) and was subjected to a treatment at 700 °C and 2 GPa for 30 min. After being taken out from the capsule, the product was crushed and washed with distilled water in an ultrasonic cleaner to remove rock salt and other chlorides. The formation of NaCl implies that the present reactions were driven by the great thermodynamical stability of this salt.

The HP synthesis of powdered  $\text{SrCo}_6\text{O}_{11}$  appears to involve exchange reactions. Cushing and Wiley reported that the hexagonal  $\text{Ca}_{x/2}\text{CoO}_2$  was easily obtained from the isostructural  $\text{Na}_x\text{CoO}_2$  through ion exchange reactions using  $\text{Ca}(\text{NO}_3)_2$  as a Ca-source and that the exchange reaction proceeded topotactically.<sup>13</sup> In the present case, the  $\text{CoO}_2$  triangular lattice of  $\gamma\text{-Na}_x\text{CoO}_2$  seems to be reconstructed into the  $\text{Co}_6\text{O}_{11}$  pillared Kagomé lattice. The transformation of  $\gamma\text{-Na}_x\text{CoO}_2 \rightarrow \text{SrCo}_6\text{O}_{11}$  (Figure 2) is not so simple as that of  $\text{Na}_x\text{CoO}_2 \rightarrow \text{Ca}_{x/2}\text{CoO}_2$ , but there is no doubt that the use of layered  $\gamma\text{-Na}_x\text{CoO}_2$  facilitated the formation of the present oxide. Experimentally, it was impossible to obtain  $\text{SrCo}_6\text{O}_{11}$  in either polycrystalline or single-crystalline form from a simple stoichiometric mixture of  $\text{SrO}$ ,  $\text{Co}_3\text{O}_4$ , and an oxidizer. We note here another example that when  $\text{PbCl}_2$  was used in place of  $\text{SrCl}_2$ , an isostructural compound  $\text{PbCo}_6\text{O}_{11}$  (hexagonal,  $a = 5.618$  Å,  $c = 12.88$  Å) was successfully obtained.

The crystal structure of  $\text{SrCo}_6\text{O}_{11}$  was determined using a crystal of  $0.20 \times 0.20 \times 0.05$  mm<sup>3</sup> in dimension. It was found to be isostructural to an *R*-type hexagonal ferrite

\* To whom correspondence should be addressed. \*Present address: Department of Chemistry, Princeton University, Princeton, NJ 08544. E-mail: ishiwata@princeton.edu.

- (1) Terasaki, I.; Sasago, Y.; Uchinokura, K. *Phys. Rev. B* **1997**, *56*, R12685–R12687.
- (2) Takada, K.; Sakurai, H.; Takayama-Muromachi, E.; Izumi, F.; Dilanian, R. A.; Sasaki, T. *Nature* **2003**, *422*, 53–55.
- (3) Ong, N. P.; Cava, R. J. *Science* **2004**, *305*, 52–53.
- (4) Ray, R.; Ghoshray, A.; Ghoshray, K.; Nakamura, S. *Phys. Rev. B* **1999**, *59*, 9454–9461.
- (5) Ishiwata, S.; Azuma, M.; Takano, M.; Nishibori, E.; Takata, M.; Sakata, M.; Kato, K. *J. Mater. Chem.* **2002**, *12*, 3733–3737.
- (6) Vander Griend, D. A.; Poeppelmeier, K. R.; Boudin, S.; Toganoh, H.; Azuma, M.; Takano, M. *J. Am. Chem. Soc.* **1998**, *120*, 11518–11519.
- (7) Gopalakrishnan, J.; Sivakumar, T.; Ramesha, K.; Thangadurai, V.; Subbanna, G. N. *J. Am. Chem. Soc.* **2000**, *122*, 6237–6241.
- (8) Schaak, R. E.; Mallouk, T. E. *Chem. Mater.* **2002**, *14*, 1455–1471.
- (9) Viciu, L.; Caruntu, G.; Royant, N.; Koenig, J.; Zhou, W. L.; Kodenkandath, T. A.; Wiley, J. B. *Inorg. Chem.* **2002**, *41*, 3385–3388.
- (10) Sivakumar, T.; Ramesha, K.; Lofland, S. E.; Ramanujachary, K. V.; Subbanna, G. N.; Gopalakrishnan, J. *Inorg. Chem.* **2004**, *43*, 1857–1864.

- (11) Dann, S. E.; Weller, M. T. *J. Solid State Chem.* **1995**, *115*, 499–507.
- (12) Motohashi, T.; Naujalis, E.; Ueda, R.; Isawa, K.; Karppinen, M.; Yamauchi, H. *Appl. Phys. Lett.* **2001**, *79*, 1480–1482.
- (13) Cushing, B. L.; Wiley, J. B. *J. Solid State Chem.* **1998**, *141*, 385–391.

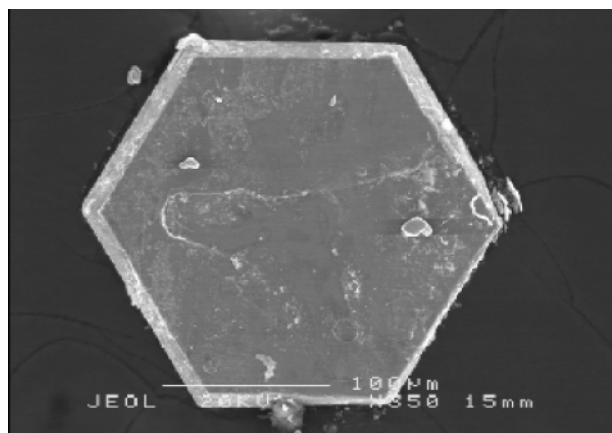


**Figure 1.** SEM image of a  $\text{SrCo}_6\text{O}_{11}$  single-crystal viewed along the  $c$ -axis. No contaminations of the Au-capsule origin were detected by the EDX analysis.

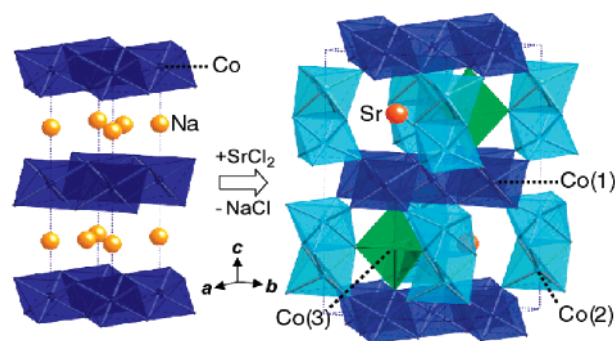


**Figure 2.** Crystal structure of  $\text{SrCo}_6\text{O}_{11}$  synthesized from  $\gamma\text{-Na}_2\text{CoO}_2$  and  $\text{SrCl}_2$  under high pressure.

**Table 1.** Refined Structural Parameters of  $\text{SrCo}_6\text{O}_{11}$  Single Crystal in the Space Group  $P6_3/mmc$  (No. 194)<sup>a</sup>

atom	site	occ.	$x$	$y$	$z$	$B/\text{\AA}^2$
Sr(1)	2c	1	1/3	2/3	1/4	0.547(6)
Co(1)	6g	1	1/2	1/2	0	0.345(3)
Co(2)	4e	1	0	0	0.14687(1)	0.354(3)
Co(3)	2d	1	2/3	1/3	1/4	0.55(1)
O(1)	12k	1	0.17471(8)	-0.17471(8)	0.08070(7)	0.58(1)
O(2)	6h	1	0.1459(1)	-0.1459(1)	0.75	0.63(2)
O(3)	4f	1	2/3	1/3	0.4198(1)	0.52(2)

<sup>a</sup>  $a = 5.609(4) \text{ \AA}$ ,  $c = 12.58(1) \text{ \AA}$ ,  $V = 342.7(5) \text{ \AA}^3$ ,  $Z = 2$ ,  $D = 5.98 \text{ g/cm}^3$ ,  $R_{\text{wp}} = 2.2\%$ ,  $R_1 = 2.3\%$ , goodness of fit indicator = 1.003.

$\text{BaTi}_2\text{Fe}_4\text{O}_{11}$  ( $P6_3/mmc$ ), which is related to the well-known magnetoplumbite structure.<sup>14</sup> The hexagonal symmetry of  $\text{SrCo}_6\text{O}_{11}$  is reflected in its external morphology shown in Figure 1. The atomic coordinates, the equivalent isotropic thermal factors, and the reliability factors are listed in Table 1. The unit cell ( $P6_3/mmc$ ,  $a = 5.609(4) \text{ \AA}$ ,  $c = 12.58(1) \text{ \AA}$ ,  $V = 342.7(5) \text{ \AA}^3$ ,  $Z = 2$ ) contains twelve cobalt ions located on three different crystallographic sites: six Co(1), four Co(2), and two Co(3). As illustrated in Figures 2 and 3, the edge-sharing  $\text{Co(1)O}_6$  octahedra form the  $\text{Co(1)}_3\text{O}_8$  Kagomé layers, while the dimerized, face-sharing octahedra of  $\text{Co(2)}_2\text{O}_9$  and the trigonal bipyramids of  $\text{Co(3)O}_5$  work as pillars parallel to the  $c$ -axis. Note that both of these pillars are arranged triangularly. The Kagomé layers and the pillars are connected with each other by corner-sharing. As far as we know, the present oxide is the first example providing

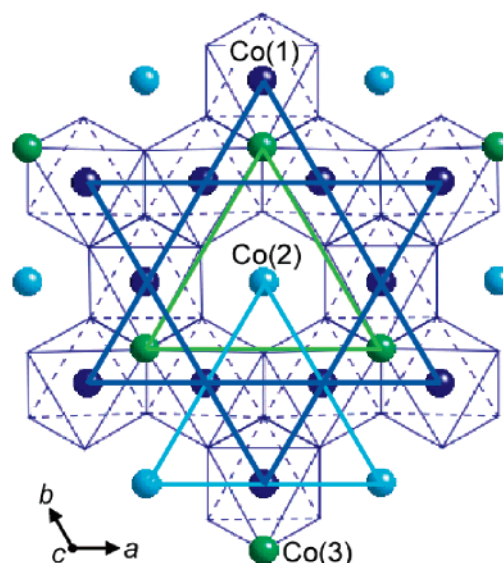


**Figure 3.** Schematic illustration of the  $\text{Co(1)}_3\text{O}_8$  Kagomé lattice viewed along the  $c$ -axis, where the triangular lattices of Co(2) and Co(3) are superimposed.

**Table 2.** Selected Bond Distances for  $\text{SrCo}_6\text{O}_{11}$

atoms	bond length/ $\text{\AA}$	atoms	bond length/ $\text{\AA}$
Co(1)–O(1) $\times 4$	1.8793(6)	Sr–O(1) $\times 6$	2.6288(8)
Co(1)–O(3) $\times 2$	1.9080(7)	Sr–O(2) $\times 6$	2.8115(7)
Co(2)–O(1) $\times 3$	1.8904(6)	Co(1)–Co(1)	2.80(4)
Co(2)–O(2) $\times 3$	1.9218(6)	Co(2)–Co(2)	2.5948(2)
Co(3)–O(2) $\times 3$	1.8204(8)		
Co(3)–O(3) $\times 2$	2.1360(10)		

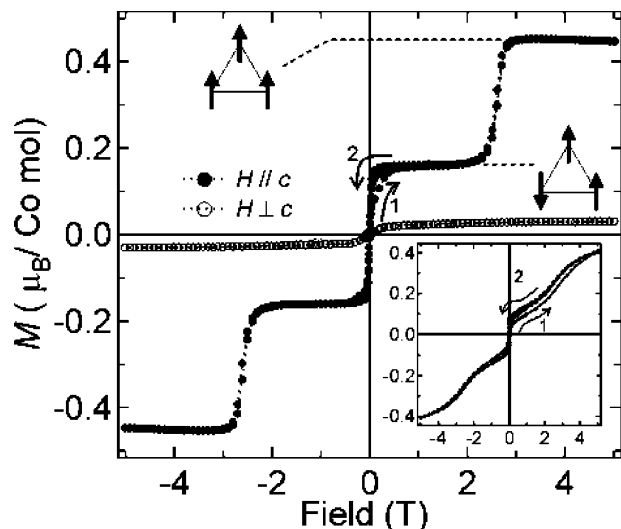
the  $\text{Co}^{3+}/\text{Co}^{4+}$ -Kagomé lattice and the trigonal bipyramidal coordination for Co ions. The Sr ions between the Kagomé layers are coordinated by twelve oxygen ions, forming  $\text{SrO}_{12}$  tetradecahedra. The selected bond distances are summarized in Table 2. When the Brown's bond valence model<sup>15</sup> was applied to these data, the oxidation states of Sr, Co(1), Co(2), and Co(3) were calculated to be +2.4, +3.6, +3.4, and +2.8, respectively. The Co(3) ions are specific in comparison with Co(1) and Co(2) with respect to coordination and valence. Considering that the d(metal) – p(oxygen) hybridization is increased as the valence of the metal ion is raised,<sup>16</sup> the  $\text{Co(1)}_3\text{O}_8$  Kagomé layer and the  $\text{Co(2)}_2\text{O}_9$  pillars containing  $\text{Co}^{4+}$  are expected to be rather conductive.

Figure 4 shows the magnetization curves of these single crystals at 5 K. When an external magnetic field,  $H$ , was applied parallel to the pillars ( $H \parallel c$ ), a relatively large magnetization ( $M_c^s = 0.45 \mu_B/\text{Co}$  or  $2.7 \mu_B/\text{formular unit}$ ) accompanied by a 1/3 plateau was observed, whereas the magnetization was quite small and linear for the field applied perpendicular to the pillars ( $H \perp c$ ). The plateau is considerably smeared out for the polycrystalline samples because the field axis and the spin axis are random to each other (see the inset of Figure 4). It is known that a hexagonal 1D system,  $\text{Ca}_3\text{Co}_2\text{O}_6$ , which comprises a triangular lattice with ferromagnetic chains at the lattice points, shows similar magnetic behavior.<sup>17,18</sup> Since the chains with strong uniaxial anisotropy along the chain axis interact antiferromagnetically

(14) Haberey, V. F.; Velicescu, M. *Acta Crystallogr.* **1974**, B30, 1507–1510.

(15) Brese, N. E.; O'Keeffe, M. *Acta Crystallogr.* **1991**, B47, 192–197.

(16) Imada, M.; Fujimori, A.; Tokura, Y. *Rev. Mod. Phys.* **1998**, 70, 1039–1263.



**Figure 4.** Magnetization curves of  $\text{SrCo}_6\text{O}_{11}$  single crystals at 5 K measured in an external magnetic field parallel (filled circle) and perpendicular (open circle) to the  $c$ -axis. The inset shows that of a polycrystalline sample at 5 K. Field-dependent hystereses are indicated by the arrows. The possible spin configurations on a triangular pillar lattice are illustrated also.

with each other,  $\text{Ca}_3\text{Co}_2\text{O}_6$  can be regarded as a triangular, frustrated Ising-like spin system. Although the spin structure in the absence of an external magnetic field remains controversial, the stepwise changes in magnetization have been interpreted as follows. When an external magnetic field is applied, the spin configuration of the chains first changes to an intermediate state like  $\uparrow\downarrow$  ( $M_c/M_c^s = 1/3$ ), and further to a ferromagnetic state like  $\uparrow\uparrow$  ( $M_c/M_c^s = 1$ ) with increasing magnetic field. Considering this example, we here assume that the 1/3 plateau in  $\text{SrCo}_6\text{O}_{11}$  stems from frustrated Ising-like spins on the  $\text{Co}(3)\text{O}_5$  pillars having triangular sublattice as schematically illustrated in Figure 4. A spin-state transition is unlikely for the stepwise magnetization within such a small energy scale ( $\sim 2.5$  T). The highly anisotropic magnetism may be expected from the relatively ionic, bipyramidally coordinated  $\text{Co}(3)$  ions rather than from the covalent,

octahedrally coordinated  $\text{Co}(1)^{3+/4+}$  and  $\text{Co}(2)^{3+/4+}$  ions in low spin state. However, the magnetic ground state of  $\text{SrCo}_6\text{O}_{11}$  remains unclear.

Isostructural compounds of  $\text{AV}_6\text{O}_{11}$  ( $A = \text{Na}, \text{K}, \text{Sr}, \text{Pb}$ ), also having uniaxial magnetic anisotropy along the  $c$ -axis, are known to undergo successive structural transitions to  $P6_3/mc$  and to  $Cmc2_1$ .<sup>19–22</sup> On the other hand, no symmetry breaking was observed by powder XRD analyses for  $\text{SrCo}_6\text{O}_{11}$  at least down to 10 K. Compared to V 3d, the stronger covalency due to the deepness of Co 3d favors high lattice symmetry, and as a result, spin frustration remains intact.

The newly found cobalt oxide  $\text{SrCo}_6\text{O}_{11}$  is novel in the sense that this is the first reported compound containing the  $\text{Co}^{3+}/\text{Co}^{4+}$ -Kagomé lattice and the unique cobalt ions with trigonal bipyramidal oxygen coordination. Additionally, the presence of the bipyramidal pillar systems furnishes unexpected magnetic features such as the 1/3 plateau in magnetization. Further details of electronic properties are now being studied using NMR and other techniques. Finally, we emphasize that the present synthetic method making use of the stability of simple salts has expanded a strategy for discovering new inspiring layered oxides at high pressure.

**Acknowledgment.** The authors thank I. Terasaki, H. Mukuda, F. Ishii, L. Viciu, and B. Muegge for helpful advice for the manuscript, and thank the MEXT of Japan for Grants-in-Aid for Scientific Research A14204070, Grants-in-Aid for COE Research on Elements Science, and Grants-in-Aid for 21<sup>st</sup> Century COE Programs at Kyoto Alliance for Chemistry.

**Supporting Information Available:** Powder XRD pattern of  $\text{SrCo}_6\text{O}_{11}$  taken at room temperature and Experimental Section including crystal growth and instrumentation. These materials are available free of charge via the Internet at <http://pubs.acs.org>.

CM050657P

- (17) Kageyama, H.; Yoshimura, K.; Kosuge, K.; Mitamura, H.; Goto, T. *J. Phys. Soc. Jpn.* **1997**, *66*, 1607–1610.  
 (18) Maignan, A.; Michel, C.; Masset, A. C.; Martin, C.; Raveau, B. *Eur. Phys. J. B* **2000**, *15*, 657–663.

- (19) Kanke, Y. *Phys. Rev. B* **1999**, *60*, 3764–3776.  
 (20) Mentre, O.; Kanke, Y.; Dhaussy, A.-C.; Conflant, P.; Hata, Y.; Kita, E. *Phys. Rev. B* **2000**, *64*, 174404.  
 (21) Kato, H.; Kato, M.; Yoshimura, K.; Kosuge, K. *J. Phys.: Condens. Matter* **2001**, *13*, 9311–9333.  
 (22) Uchida, Y.; Onoda, Y.; Kanke, Y. *J. Magn. Magn. Mater.* **2001**, *13*, 446–448.